Proc. Natl. Acad. Sci. USA
Vol. 85, pp. 4056–4060, June 1988
Neurobiology

Electrophysiological characterization of cloned m1 muscarinic receptors expressed in A9 L cells

(ion channels/Ca^{2+}-dependent K^+ conductance/cDNA/fibroblast/Ca^{2+}-dependent Cl^- conductance)

S. V. PENELOPE JONES*, JEFFERY L. BARKER*, TOM I. BONNER†, NOEL J. BUCKLEY†, AND MARK R. BRANN‡§

*Laboratory of Neurophysiology, National Institute of Neurological and Communicative Disorders and Stroke, †Laboratory of Cell Biology, National Institute of Mental Health, and ‡Metabolic Diseases Branch, National Institute of Diabetes, Digestive and Kidney Diseases, National Institutes of Health, Bethesda, MD 20892

Communicated by M. Nirenberg, January 4, 1988

ABSTRACT **The electrophysiological properties of A9 L cells stably transfected with m1 muscarinic receptor cDNA were examined by using the whole-cell patch-clamp technique. In current-clamp recordings, acetylcholine (AcCho) elicited a hyperpolarization of all transfected cells studied but had no effect on nontransfected A9 L cells. In voltage-clamp recordings, AcCho elicited an outward current at −50 mV accompanied by an increase in conductance. The onset of the current response was consistently delayed by several seconds with respect to the onset of the application of AcCho and could not be accounted for by diffusion. The AcCho-induced currents were reversibly inhibited by the muscarinic receptor antagonist atropine (1 μM) but were unaffected by the nicotinic receptor antagonist tubocurarine (50 μM). Ion-substitution experiments replacing K^+ with *N*-methyl-D-glucamine and Cl^- with methanesulfonate indicated that the current was carried mainly by K^+, although a minor part appeared to be carried by Cl^-. The AcCho-induced current could be blocked by the K^+ channel blocking agents tetraethylammonium ion, 4-aminopyridine, apamin, and Ba^{2+} but not by Cs^+. The AcCho-induced current was inhibited when 5 mM 1,2-bis(2-aminophenoxy)ethane-*N*,*N*,*N*′,*N*′-tetraacetic acid (BAPTA) was included in the patch pipette or when extracellular Cd^{2+} or Co^{2+} was applied, indicating a role for intracellular Ca^{2+} in the generation of the response. Thus, these results show that cloned m1 muscarinic receptors expressed in A9 L cells can activate a Ca^{2+}-dependent K^+ conductance, possibly via a second-messenger system.**

Stimulation of muscarinic receptors by the neurotransmitter acetylcholine (AcCho) or by cholinergic agonists such as muscarine or carbachol leads to a complex spectrum of signals involving various transduction mechanisms. The responses to muscarinic receptor stimulation include inhibition of adenylate cyclase, stimulation of GTPase and guanylate cyclase, enhanced phospholipid turnover, increased cAMP-dependent phosphodiesterase activity, and modulation of ion channel activity (reviewed in refs. 1–3).

The effects of muscarinic-receptor stimulation on ion channel activity can be divided into hyperpolarizing and depolarizing responses mediated mostly through changes in either voltage- or Ca^{2+}-dependent K^+ conductances. Attempts to categorize the responses to muscarinic receptor stimulation using ligand binding techniques have divided the muscarinic responses into M1 and M2 muscarinic receptor subtypes based on high (M1) and low (M2) affinity for pirenzepine (4). Electrophysiological experiments have attempted to associate specific functions with the receptor subtypes defined biochemically. For example, North *et al.* (5) distinguished presynaptic (M2) and postsynaptic (M1) muscarinic receptors in guinea pig intestinal smooth muscle. M1 muscarinic receptor stimulation of hippocampal and cortical neurons depolarized cells by inhibiting a voltage-dependent K^+ conductance (6, 7), whereas M2 muscarinic receptor stimulation depolarized supraspinal neurons apparently by two other mechanisms (7): (*i*) by inhibiting the action-potential after-hyperpolarization, presumably because of inhibition of a Ca^{2+}-dependent K^+ conductance (8), and (*ii*) by activating a depolarizing conductance (6). Other investigations in different supraspinal neurons have revealed yet other electrophysiological responses to M2 receptor stimulation (9, 10). Thus, this diversity of electrical signals strongly suggests that there are more than two muscarinic receptor subclasses regulating various transduction mechanisms.

Attempts to identify specific signal transduction mechanisms associated with M1 and M2 receptors were made initially by injecting mRNAs from a variety of organs expressing muscarinic receptors into *Xenopus* oocytes. Muscarinic receptors translated from rat small intestine mRNA were found to couple to a whole spectrum of hyperpolarizing and depolarizing responses (11). Injection of rat brain mRNA into *Xenopus* oocytes yielded only a chloride-dependent depolarizing response (12). The cloning of two distinct muscarinic receptor cDNAs, one from porcine brain (13) and one from porcine heart (14), has begun to allow resolution of muscarinic receptor functions associated with clonally derived subtypes. Bonner *et al.* (15) have cloned the human and rat homologs of these muscarinic receptor subtypes as well as two additional receptor subtypes cloned from rat brain. These four muscarinic receptor cDNAs have been designated m1–m4 based on the chronological order of determination of their primary sequences.

In an initial study by Kubo *et al.* (13), the mRNA obtained from a muscarinic-receptor cDNA, cloned from porcine brain (m1), was injected into *Xenopus* oocytes. Cholinergic stimulation of the m1 receptor activated a Ca^{2+}-dependent Cl^- conductance, whereas stimulation of the muscarinic receptor cloned from porcine heart (m2) when expressed in *Xenopus* oocytes activated a Ca^{2+}-dependent Cl^- conductance and a nonspecific cationic conductance (16); the latter response has only been seen previously in recordings from smooth muscle (17). We have used a strategy involving the stable transfection of mammalian cell lines with each of the muscarinic receptor cDNAs to examine some of the details involved in the expression and cellular functions of the different receptors (18). The present study uses the tight-seal whole-cell

The publication costs of this article were defrayed in part by page charge payment. This article must therefore be hereby marked "*advertisement*" in accordance with 18 U.S.C. §1734 solely to indicate this fact.

Abbreviations: AcCho, acetylcholine; NMeGCl, *N*-methylglucamine chloride; $NMeGMeSO_3$, *N*-methyl-D-glucamine methanesulfonate; BAPTA, 1,2-bis(2-aminophenoxy)ethane-*N*,*N*,*N*′,*N*′-tetraacetic acid.

§Present address: Laboratory of Molecular Biology, National Institute of Neurological and Communicative Disorders and Stroke, Building 36, Room 3D02, NIH, Bethesda, MD 20892.

recording technique to examine the electrophysiological consequences of muscarinic receptor stimulation in A9 L cell fibroblasts transfected with the m1 receptor cDNA cloned from rat brain. This receptor is the rat homolog of the receptor (cloned from porcine brain) studied by Kubo *et al.* in *Xenopus* oocytes (13). The m1 receptor of the present study has high affinity for pirenzepine and previously would have been placed in the M1 subclass. A preliminary investigation indicated that the m1 muscarinic receptor cDNA-transfected cells produce electrically detectable, atropine-sensitive responses to AcCho (18).

MATERIALS AND METHODS

A9 L cells were transfected with the m1 muscarinic receptor cDNA (18), and single clones were isolated at limiting dilution. The cells were maintained in culture in 3-cm Petri dishes in Dulbecco's modified Eagle's medium containing 10% (vol/vol) fetal bovine serum at 37°C in 95% air/5% CO_2 for at least 24 hr. Cells were studied at room temperature (20–24°C) on the inverted stage of a phase-contrast microscope at a magnification of ×320. The tight-seal whole-cell recording technique was used to record membrane currents and potentials with a LIST EPC-7 amplifier (19). The patch electrodes were made from thin-wall capillary borosilicate glass (W-P Instruments, New Haven, CT) and pulled on a two-stage horizontal electrode puller (Mecanex, Basel, Switzerland). Pipette resistances were 4–10 MΩ when placed in the bath and varied with pipette solution. Pipette seals of between 5 and 20 GΩ were obtained before disruption of the membrane patch. Once access to the cell interior was established, cell input resistances of 1–3 GΩ were obtained at resting potential (approximately −50 mV). Series resistance compensation was applied in voltage-clamp.

The extracellular medium was composed of 140 mM NaCl, 5 mM KCl, 5 mM Hepes, 5.6 mM D-glucose, 2 mM $CaCl_2$, and 1 mM $MgCl_2$ (pH adjusted to 7.4 with NaOH). The osmolarity was adjusted to 330–335 mosM with sucrose. Other extracellular solutions used include a K^+ medium containing 70 mM potassium gluconate, 70 mM *N*-methyl-D-glucamine methanesulfonate ($NMeGMeSO_3$), 5 mM Hepes, 2 mM $CaCl_2$, 1 mM $MgCl_2$, and 5.6 mM glucose (pH adjusted to 7.4 with KOH). In most experiments the intracellular patch pipette solution contained 150 mM potassium gluconate, 2 mM $MgCl_2$, 5 mM Hepes, 1.1 mM EGTA, 0.1 mM $CaCl_2$, 5 mM Mg-ATP, and 0.1 mM Li-GTP (pH adjusted to 7.2 with KOH). The osmolarity was adjusted to 320–325 mosM with sucrose. The free Ca^{2+} concentration was estimated to be about 20 nM (20). Other solutions used included a KCl-containing solution in which 150 mM potassium gluconate was replaced by 150 mM KCl and an intracellular $NMeGMeSO_3$-containing solution in which potassium gluconate was replaced with 150 mM $NMeGMeSO_3$. Liquid-junction potentials between the bath solution and intracellular electrode solutions were eliminated by filling a side bath containing the reference electrode with the intracellular solution. Connections between the two baths were made via a low-resistance bridge.

Current-clamp recordings were made at resting potential, and a series of 100-ms currents were injected in 10-pA steps in both hyperpolarizing and depolarizing directions at a frequency of 1 Hz. Membrane currents were usually recorded from cells voltage-clamped at −50 mV. Either resting current measurements were taken or the currents produced by a series of 10-mV, 100-ms hyperpolarizing and depolarizing voltage steps applied at a frequency of 1 Hz were recorded. AcCho (10–50 μM) was applied by low (1–2 psi; 1 psi = 6.89 kPa) pressure from a micropipette placed 5–10 μm from the cell. AcCho pulses were usually applied at 3-min intervals, as this was sufficient to evoke constant-amplitude current responses. The current and voltage responses were displayed on a Gould pen recorder (filtered at 50 Hz) and also sampled and digitized on-line by a PDP 11/23 minicomputer with an analogue-to-digital Data Translation converter (12 bit, ±5-V range), at a digitization rate of 2.5 kHz. Signals were filtered at 1 kHz. Antagonists were applied directly to the bath, and solution changes were obtained by perfusion of the 1.5-ml bath with fresh medium at a flow rate of 2 ml·min^{-1}. All results are expressed as means ± SEM.

RESULTS

Responses of Transfected A9 L Cells to Muscarinic Agonists. Resting membrane potentials of −52 ± 1 mV (n = 76) were obtained on first breaking into cells transfected with m1 muscarinic receptor cDNA. This resting level is in a similar range to that obtained in nontransfected A9 L cells and to resting potentials measured in L cells by Hosoi and Slayman (21). Application of 10–50 μM AcCho consistently produced a hyperpolarization of ≈25 mV and eliminated the low-amplitude membrane potential fluctuations evident at the resting potential (Fig. 1*A*). The onset of the hyperpolarization was characteristically delayed by about 3 s after the commencement of AcCho application. The delay was not due to time required for diffusion of AcCho from the micropipette to the cell surface because application of elevated K^+ (150 mM) depolarized cells within 50 ms. The voltage responses to a series of current injections from the resting potential are shown in Fig. 1*B*. Injection of currents into the cell generated simple charging curves over a 160-mV range of membrane potential with no evidence of time- or voltage-dependent conductance mechanisms. Application of AcCho to transfected cells markedly attenuated the voltage responses, indicating that the hyperpolarizing response was accompanied by an increase in membrane resistance (Fig. 1*B*). These effects on membrane properties have been studied under voltage-clamp. Current–voltage (*I–V*) relationships obtained under control conditions revealed a linear relationship over the range −100 to +60 mV, thus showing no evidence of voltage-activated conductances (Fig. 2). Application of Ac-

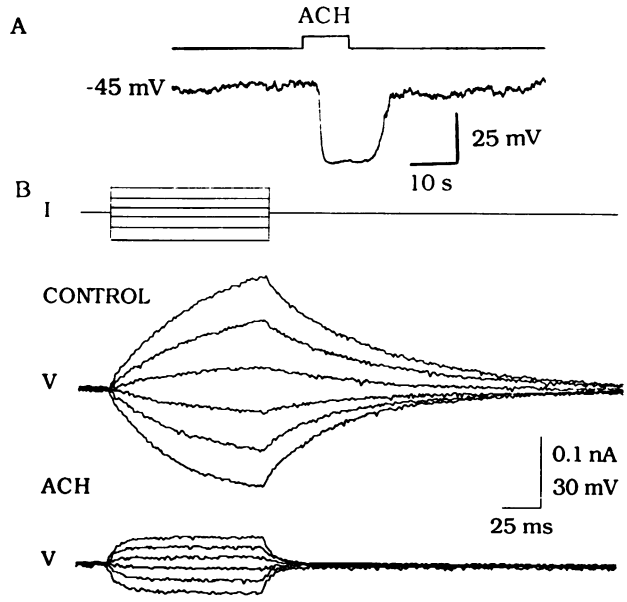

FIG. 1. AcCho hyperpolarizes A9 L cells transfected with the m1 muscarinic receptor cDNA and decreases their input resistance. Current-clamp recordings of A9 L cells in physiological saline with potassium gluconate as the intracellular electrolyte are shown. (*A*) AcCho (50 μM) applied by low pressure during the period indicated hyperpolarizes an A9 L cell after about a 3-s delay. (*B*) The cell was current-clamped at −50 mV, and 100-ms hyperpolarizing and depolarizing current steps of 10-pA increments (line I) were injected under control conditions and in the presence of 50 μM AcCho. A marked decrease in all of the voltage responses is evident in the presence of AcCho.

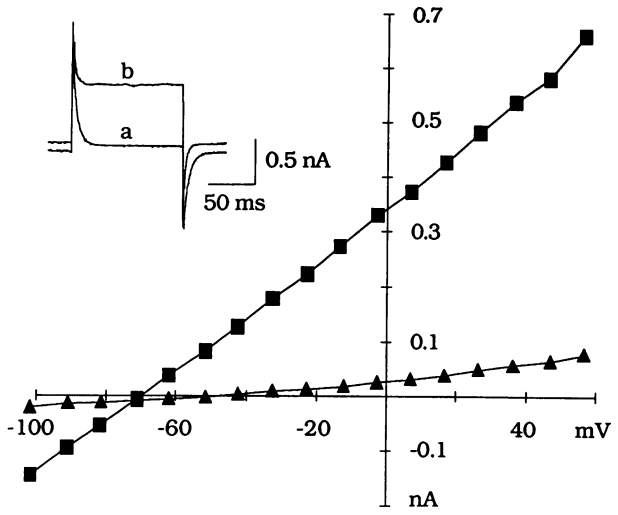

FIG. 2. AcCho alters the current-voltage (*I–V*) curve of an A9 L cell transfected with the m1 muscarinic receptor. Representative *I–V* relationship for 100-ms voltage steps in the absence (▲) and presence of 50 μM AcCho (■), measured at the end of the 100-ms step. (*Inset*) Digitized current response to a voltage step from −50 mV to +60 mV in the absence (trace a) and presence (trace b) of AcCho. Downward deflections denote inward current. The experiment was carried out in physiological saline with potassium gluconate as the intracellular electrolyte. AcCho alters the slope conductance from 0.4 nS to 4.4 nS. In the presence of AcCho, the *I–V* curve intersects 0 nA at −70 mV, the reversal potential for the response.

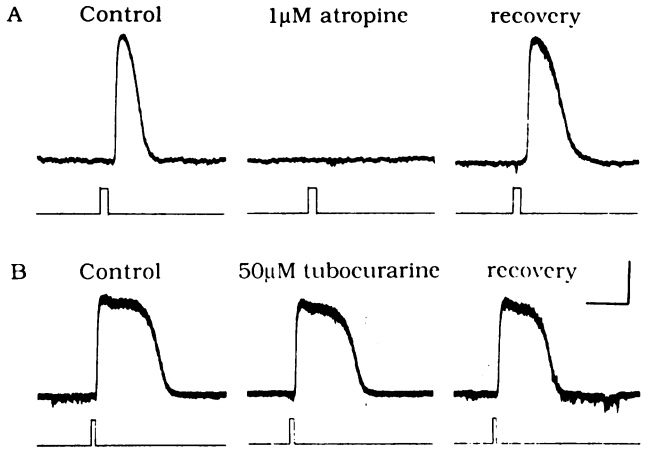

FIG. 3. (*A*) Atropine inhibits the AcCho-induced current responses in A9 L cells transfected with the m1 muscarinic receptor cDNA. Cells were voltage-clamped at −50 mV. Responses are shown before and 5 min after the addition of 1 μM atropine. Recovery was complete 10 min after washing with fresh bathing solution. (*B*) AcCho-induced current responses are unaffected by tubocurarine (50 μM). In both *A* and *B* the upper traces show current responses to pulses of AcCho (50 μM). An upward deflection denotes outward current. The lower traces show application of AcCho. Vertical calibration denotes 35 pA; horizontal calibration denotes 10 s in *A* and 20 s in *B*.

Cho reduced input resistance from 2.7 ± 0.5 to 0.3 ± 0.1 GΩ (n = 10) and correspondingly increased the slope conductance 8-fold, from 0.5 ± 0.1 to 4.3 ± 0.9 nS (n = 10). The *I–V* relationship remained linear over the 160-mV range of potentials in the presence of AcCho (Fig. 2). The kinetics of the membrane current responses to various voltage steps were similar under control conditions and in the presence of AcCho, showing no evidence of inactivation during voltage steps of up to 500 ms at any potential tested. At −50 mV the current was outward in direction and delayed in onset after the application of AcCho (Fig. 3). An increase in current noise accompanied the outward response. Carbachol (100 μM) applied to the bathing medium also elicited a delayed outward current at −50 mV, associated with an increase in membrane conductance (not shown). Responses of transfected A9 L cells to AcCho ran down after several applications unless the patch pipettes were filled with a solution that contained both ATP and GTP. It should be noted that A9 L cells not transfected with the m1 receptor cDNA did not respond to AcCho in an electrically detectable manner (n = 10). Furthermore, extracellular medium elicited no responses in transfected cells (n = 3).

Effects of Nicotinic and Muscarinic Antagonists. The AcCho-induced responses were reversibly inhibited by the muscarinic receptor antagonist atropine (1 μM) (Fig. 3*A*). Atropine had no effect on resting membrane potential nor on the *I–V* relationship of the cell. The nicotinic receptor antagonist tubocurarine (50 μM) had no effect on the AcCho-induced responses (Fig. 3*B*).

Ionic Mechanism of AcCho-Induced Conductance. The AcCho-induced currents reversed in polarity at −67 ± 3 mV (n = 5) when recorded with pipettes containing the basic potassium gluconate solution (Fig. 2). Using the Nernst equation

$$E_{ion} = \frac{RT}{ZF} \log_e [ion]_{out}/[ion]_{in}$$

in which E_{ion} is the equilibrium potential for that ion, Z is the valency of the ion, R is the gas constant, F is the Faraday constant, and T is the temperature in degrees Kelvin, we calculated the equilibrium potential (i.e., the potential at which there is no net current flow) for these recording conditions to be −86 mV for K^+ (E_K) and −92 mV for Cl^- (E_{Cl}). When the cells were dialyzed with 150 mM KCl instead of 150 mM potassium gluconate, the AcCho-induced current reversed at −80 ± 5 mV (n = 5) (Fig. 4*A*). Although E_K calculated under these conditions remained −86 mV, E_{Cl} became 0 mV. Thus, the AcCho-induced current appears to be carried mainly by K^+. Differences in reversal potentials between the two solutions can be explained in terms of differences in the liquid-junction potentials between the pipette solutions and the cells' physiological intracellular composition.

When current responses to AcCho were recorded from cells dialyzed with an $NMeGMeSO_3$-containing solution and in a medium containing 70 mM K^+, where E_K was made positive to 0 mV, E_{AcCho} also became positive (Fig. 4*B*). After the effects of AcCho in the K^+-containing solution were measured, the cells were superfused with a K^+-free medium substituted with 140 mM $NMeGMeSO_3$. Under these conditions responses were not detectable, suggesting that neither NMeG nor $MeSO_3$ could carry the current. Upon reversion to the K^+-containing medium, the AcCho-induced currents were recovered (not shown). The slope conductance determined in the K^+-containing extracellular solution was increased 8-fold from 0.3 ± 0.1 obtained in control to 2.4 ± 0.6 nS (n = 3) obtained during application of AcCho. When cells were dialyzed with the $NMeGMeSO_3$-containing solution and bathed in a 140-mM NMeGCl, the AcCho-induced current reversed in polarity at −101 ± 6 mV (n = 3) (Fig. 4*C*). E_{Cl} was calculated to be −92 mV in this solution, indicating that the AcCho-induced current could also be carried by Cl^-. However, the slope conductance only increased 2-fold from 0.2 ± 0.1 in the control to 0.4 ± 0.1 nS (n = 3) in the presence of 50 μM AcCho.

During exchange of the extracellular medium from one containing K^+ to one containing Cl^-, when the extracellular medium was transiently composed of K^+ and Cl^-, a biphasic current response was observed (Fig. 4*D*, middle trace). This consisted of an initial inward component, presumably carried by K^+, followed by an outward component of larger amplitude, presumably reflecting Cl^- flux. After a relatively complete

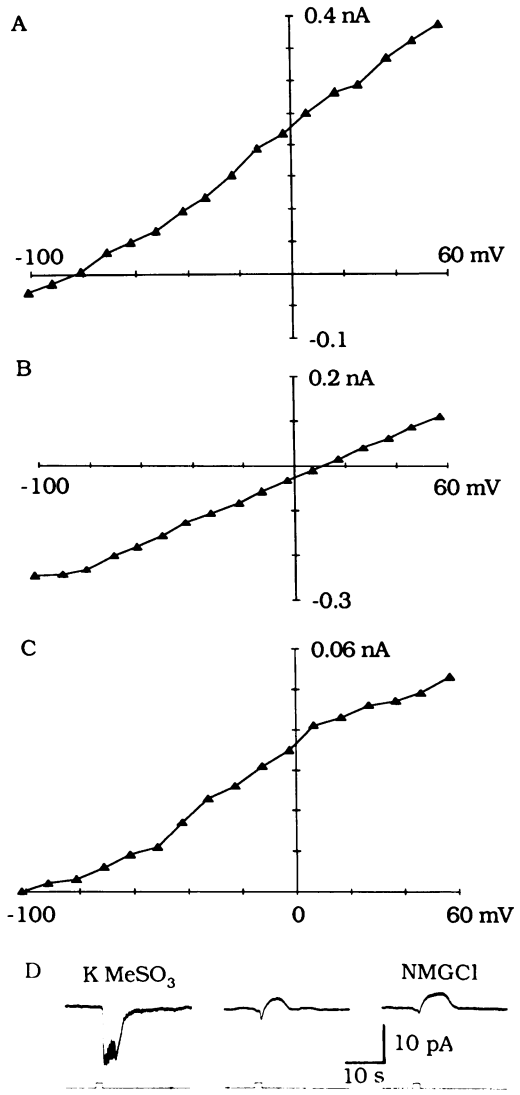

FIG. 4. AcCho-induced response reverses polarity according to K^+ and Cl^- gradients. Leak-subtracted (AcCho *I–V* minus control *I–V*) representative *I–V* curves to 100-ms voltage steps from a holding potential of −50 mV are plotted for different recording conditions. Currents were measured at the end of the 100-ms steps. (*A*) Recorded in physiological medium with KCl as the intracellular electrolyte (reversal potential, −80 mV; slope conductance, 2.8 nS). (*B*) Recorded in 70 mM potassium gluconate/70 mM $NMeGMeSO_3$ in the extracellular medium and $NMeGMeSO_3$ in the intracellular pipette solution (reversal potential, +10 mV; slope conductance, 2.5 nS). (*C*) Recorded in *N*-methylglucamine chloride (NMeGCl) extracellular medium and $NMeGMeSO_3$ intracellular pipette solution (reversal potential, −100 mV; slope conductance, 0.35 nS). (*D*) AcCho-induced currents recorded at −50 mV, initially in an extracellular solution containing 140 mM potassium methanesulfonate ($KMeSO_3$; left trace), followed by the AcCho-induced currents recorded during the exchange of medium from $KMeSO_3$ to one containing 140 mM NMeGCl (NMGCl; right trace). The intracellular solution contained $NMeGMeSO_3$. An upward deflection denotes outward current in the upper trace. The lower trace shows application of AcCho.

exchange of Cl^- for the K^+-containing medium, the inward (K^+) current was virtually abolished and the outward (Cl^-) current increased in size. Thus, both K^+ and Cl^- can be conducted across the membrane after application of AcCho.

Pharmacology of AcCho-Induced Currents. Various agents known to block depolarization-activated K^+ conductances, including tetraethylammonium ion (not shown), 4-aminopyridine (not shown), and Ba^{2+} (Fig. 5*A*), reversibly depressed or abolished the AcCho-induced K^+ currents [tetraethylammonium ion (1 mM) and 4-aminopyridine (3 mM) also bind to the muscarinic receptor; unpublished results]. However, Cs^+, which blocks hyperpolarization-activated K^+ conductances, did not affect the AcCho-induced K^+ current (Fig. 5*B*). Apamin, a bee venom toxin that blocks Ca^{2+}-dependent K^+ conductances (22), also eliminated the responses to AcCho (Fig. 5*C*), suggesting that activation of the K^+ conductance could require Ca^{2+}. This was supported by depression of the AcCho-induced currents by the divalent cations Co^{2+} (not shown) and Cd^{2+} (Fig. 5*D*), which block depolarization-activated and hormone-induced Ca^{2+} entry. A role for intracellularly located Ca^{2+} was suggested by the loss of current responses to AcCho in cells dialyzed with 5 mM BAPTA instead of 1.1 mM EGTA ($n = 6$) (Fig. 5*E*). BAPTA acts rapidly to buffer intracellular Ca^{2+} levels (23).

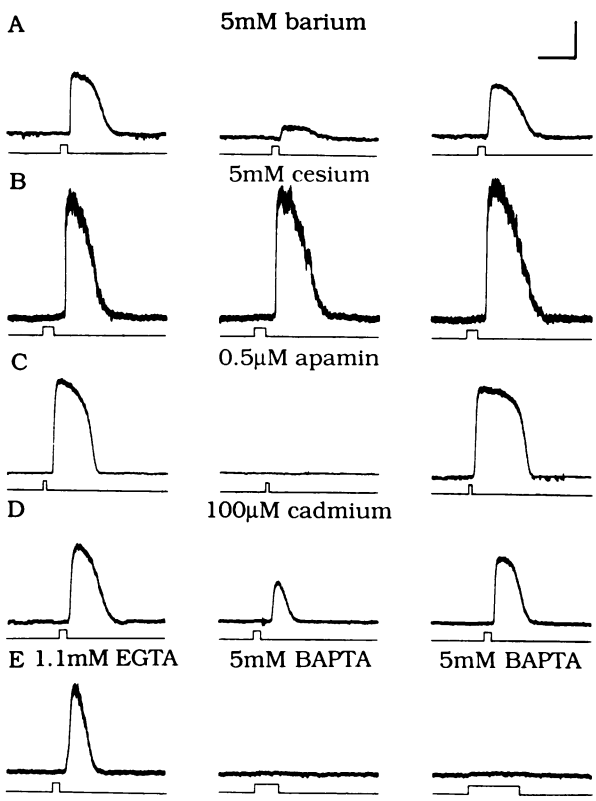

FIG. 5. AcCho-induced currents are reduced or abolished by K^+ channel blocking agents or by maneuvers that block increases in intracellular Ca^{2+} concentration. Current responses evoked by AcCho (50 μM) were recorded under voltage-clamp at −50 mV in physiological saline with potassium gluconate as the intracellular electrolyte. (*Left*) Control responses. (*Center*) Responses ≈5 min after addition of drug to the bathing medium. (*Right*) Recovery of the responses after the drug was washed out. (*A–E*) Upper traces show AcCho-induced currents, and lower traces show application of 50 μM AcCho. The AcCho-induced current is attenuated in a reversible manner by 5 mM Ba^{2+} (*A*), is unaffected by 5 mM Cs^+ (*B*), and is eliminated by 0.5 μM apamin (*C*). Cd^{2+} (100 μM) reduced the AcCho-induced current (*D*). (*E*) Responses to AcCho recorded in two different cells with patch pipette solutions containing either 1.1 mM EGTA (used in all other experiments) or 5 mM 1,2-bis(2-aminophenoxy)ethane-*N*,*N*,*N*′,*N*′-tetraacetic acid (BAPTA) as the Ca^{2+} chelator. The currents recorded with BAPTA are from the same cell and show no response to AcCho with two different durations of AcCho application. Horizontal calibration denotes 10 s except in *C* where it denotes 20 s. Vertical calibration denotes 50 pA except in *B* where it denotes 10 pA.

DISCUSSION

The cloned m1 muscarinic receptor was expressed in A9 L cells in order to characterize the function of the m1 receptor in isolation from the other muscarinic receptor subtypes. A9

L cells not transfected with the m1 muscarinic receptor cDNA do not bind the muscarinic receptor antagonist quinuclidinyl benzilate nor respond to AcCho, which suggests that they do not have endogenous muscarinic receptors. Therefore, they are potential model cells for studying muscarinic receptor expression and function. The results of the present electrophysiological characterization of the m1 muscarinic receptor show that AcCho hyperpolarizes the A9 L cell membrane. This hyperpolarization is induced by an increase in membrane conductance primarily due to K^+ and secondarily to Cl^-. The increase in conductance is characteristically delayed with respect to application of AcCho by several seconds, much longer than could be accounted for simply by diffusion of AcCho from pipette to cell surface. Several seconds of application of AcCho evoked responses lasting tens of seconds. The response is muscarinic, since it is eliminated by the muscarinic receptor antagonist atropine but not by the nicotinic receptor antagonist tubocurarine. Most of the ionic conductance is attenuated by substances that either block K^+ conductances or effectively limit rapid increases in intracellular Ca^{2+} concentration. These results imply that stimulation of m1 muscarinic receptors increases intracellular Ca^{2+}, which in turn activates predominantly a K^+ conductance and to a lesser extent a Cl^- conductance. The predominance of the K^+ conductance over the Cl^- conductance may be due to the sensitivity of the channels to internal Ca^{2+}. Marty *et al.* (24) found that Ca^{2+}-dependent K^+ channels in lacrimal glands are activated by lower concentrations of Ca^{2+} than those that activate the Ca^{2+}-dependent Cl^- channels.

As the activation of the Ca^{2+}-dependent K^+ channel in response to AcCho application was delayed by several seconds, a second messenger system is probably being stimulated to increase the intracellular Ca^{2+} concentration. Such a mediator might be inositol 1,4,5-trisphosphate [Ins-(1,4,5)P_3] which releases Ca^{2+} from intracellular stores. Inositol metabolism has been associated with one of the many effects of muscarinic receptor stimulation, and Ins(1,4,5)P_3 has been shown in *Xenopus* oocytes to mimic AcCho receptor stimulation and to activate a Ca^{2+}-dependent Cl^- conductance (25). Ins(1,4,5)P_3 also activated the Ca^{2+}-dependent Cl^- and Ca^{2+}-dependent K^+ conductances in rat lacrimal glands (26). As predicted, phosphatidylinositol turnover is stimulated by AcCho in m1 muscarinic receptor cDNA-transfected A9 L cells to produce Ins(1,4,5)P_3 (unpublished observations).

The Ca^{2+}-dependent K^+ and Cl^- conductances activated in A9 L cells by m1 muscarinic-receptor stimulation are comparable to the Ca^{2+}-dependent K^+ and Cl^- conductances activated by muscarinic-receptor stimulation in lacrimal glands (26) and to the Ca^{2+}-dependent K^+ conductance of submandibular glands (27). The results of this study differ from those of Kubo *et al.* (13) in which stimulation of the m1 muscarinic receptor activated only a Ca^{2+}-dependent Cl^- conductance in *Xenopus* oocytes.

While m1 muscarinic receptors are abundant in the central nervous system, no stimulation of Ca^{2+}-dependent K^+ channels has been demonstrated there. Thus, it is likely that m1 receptors exert electrical effects not observed in A9 L cells. Since A9 L cells are derived from peripheral endothelial tissue, they may not possess the complement of messengers and effectors required to produce a neuronal type of response. This is borne out by the absence in A9 L cells of the signal transducing GTP-binding proteins G_o and G_{i1} (unpublished observations) (G_{i1} is referred to as $G_{i\alpha}$ in ref. 28), which are only found in neuronal cells (29). Transfection of the A9 L cells with both m1 muscarinic receptor cDNA and one of these GTP-binding proteins may result in a neuronal type of response to m1 muscarinic receptor stimulation. Alternatively, neuronal cells may be used as hosts for transfection of m1 receptors.

The above method of transfecting a known cell line with each of the different muscarinic receptor subtypes will help to answer numerous questions related to the molecular basis of the muscarinic response. Correlation of the response of a cell to muscarinic receptor stimulation to the receptor subtype, determination of the GTP-binding proteins available within the cell, and what second messenger systems may be activated can be established by using transfection methods. These variables also can be related to which channels are present within a cell and how they are modulated by receptors.

This study shows that the A9 L cell provides an excellent model for determining the mechanism of the m1 muscarinic receptor in that it contains the complete pathway to activate a channel that seems to replicate a known physiological response of muscarinic-receptor stimulation. Whether these cells also contain the pathways necessary for other muscarinic-receptor subtypes remains to be seen.

We thank Drs. M. J. Brownstein and A. Spiegel for their support and Dr. R. M. Collins for assistance.

1. Nathanson, N. M. (1987) *Annu. Rev. Neurosci.* **10**, 195–236.
2. Brown, D. (1986) *Nature (London)* **319**, 358–359.
3. Harden, T. K., Tanner, L. I., Martin, M. W., Nakahata, N., Hughes, A. R., Hepler, J. R., Evans, T., Masters, S. B. & Brown, J. H. (1986) *Trends Pharmacol. Sci.* **7**, Suppl., 14–18.
4. Hammer, R., Berrie, C. P., Birdsall, N. J. M., Burgen, A. S. V. & Hulme, E. C. (1980) *Nature (London)* **283**, 90–92.
5. North, R. A., Slack, B. E. & Surprenant, A. (1985) *J. Physiol. (London)* **368**, 435–452.
6. McCormick, D. A. & Prince, D. A. (1985) *Proc. Natl. Acad. Sci. USA* **82**, 6344–6348.
7. Muller, W. & Misgeld, U. (1986) *Neurosci. Lett.* **67**, 107–112.
8. Madison, D. V., Lancaster, B. & Nicoll, R. A. (1987) *J. Neurosci.* **7**, 733–741.
9. Egan, T. M. & North, R. A. (1986) *Nature (London)* **319**, 405–407.
10. McCormick, D. A. & Prince, D. A. (1986) *Nature (London)* **319**, 402–405.
11. Aoshima, H., Iio, H., Anan, M., Ishii, H. & Kobayashi, S. (1987) *Mol. Brain Res.* **2**, 15–20.
12. Sugiyama, H., Hisanaga, Y. & Hirono, C. (1985) *Brain Res.* **388**, 346–350.
13. Kubo, T., Fukuda, K., Mikami, A., Maeda, A., Takahashi, H., Mishina, M., Haga, T., Ichiyama, A., Kangawa, K., Kojima, M., Matsuo, H., Hirose, T. & Numa, S. (1986) *Nature (London)* **323**, 411–416.
14. Kubo, T., Maeda, A., Sugimoto, K., Akiba, I., Mikami, A., Takahashi, H., Haga, T., Haga, K., Ichiyama, A., Kangawa, K., Matsuo, H., Hirose, T. & Numa, S. (1987) *FEBS Lett.* **209**, 367–372.
15. Bonner, T. I., Buckley, N. J., Young, A. C. & Brann, M. R. (1987) *Science* **237**, 527–532.
16. Fukuda, K., Kubo, T., Akiba, I., Maeda, A., Mishina, M. & Numa, S. (1987) *Nature (London)* **327**, 623–625.
17. Benham, C. D., Bolton, T. B. & Lang, R. J. (1985) *Nature (London)* **316**, 345–346.
18. Brann, M. R., Buckley, N. J., Jones, S. V. P. & Bonner, T. I. (1987) *Mol. Pharmacol.* **32**, 450–455.
19. Hamill, O. P., Marty, A., Neher, E., Sakmann, B. & Sigworth, F. (1981) *Pflügers Arch.* **391**, 85–100.
20. Abercrombie, R. F., Masukawa, L. M., Sjodin, R. A. & Livengood, D. (1981) *J. Gen. Physiol.* **78**, 413–429.
21. Hosoi, S. & Slayman, C. L. (1985) *J. Physiol. (London)* **367**, 267–290.
22. Blatz, A. L. & Magleby, K. L. (1986) *Nature (London)* **323**, 718–720.
23. Tsien, R. Y. (1983) *Annu. Rev. Biophys. Bioeng.* **12**, 91–116.
24. Marty, A., Evans, M. G., Tan, Y. P. & Trautmann, A. (1986) *J. Exp. Biol.* **124**, 15–32.
25. Oron, Y., Dascal, N., Nadler, E. & Lapu, N. (1985) *Nature (London)* **313**, 141–143.
26. Evans, M. G. & Marty, A. (1986) *Proc. Natl. Acad. Sci. USA* **83**, 4099–4103.
27. Gallacher, D. V. & Morris, A. P. (1987) *J. Physiol. (London)* **384**, 119–130.
28. Nukada, T., Tamabe, T., Takahashi, H., Noda, M., Haga, K., Haga, T., Ichiyana, A., Kangawa, K., Hiranaga, M., Matsuo, H. & Numa, S. (1986) *FEBS Lett.* **197**, 305–310.
29. Brann, M. R., Collins, R. M. & Spiegel, A. (1987) *FEBS Lett.* **222**, 191–198.